

Lower bound on the spread of valley splitting in Si/SiGe quantum wells induced by atomic rearrangement at the interface

Gang Wang(王刚), Shan Guan(管闪) Zhi-Gang Song(宋志刚) and Jun-Wei Luo(骆军委)
Citation: Chin. Phys. B, 2023, 32 (**10**): 107309. DOI: 10.1088/1674-1056/acf208
Journal homepage: http://cpb.iphy.ac.cn; http://iopscience.iop.org/cpb

What follows is a list of articles you may be interested in

Dispersion of exciton-polariton based on ZnO/MgZnO quantum wells at room temperature

Huying Zheng(郑湖颖), Zhiyang Chen(陈智阳), Hai Zhu(朱海), Ziying Tang(汤梓荧), Yaqi Wang(王亚琪), Haiyuan Wei(韦海园), Chongxin Shan(单崇新)
Chin. Phys. B, 2020, 29 (**9**): 097302. DOI: 10.1088/1674-1056/ab99b3

Enhanced spin-dependent thermopower in a double-quantum-dot sandwiched between two-dimensional electron gases

Feng Chi(迟锋), Zhen-Guo Fu(付振国), Liming Liu(刘黎明), Ping Zhang(张平)
Chin. Phys. B, 2019, 28 (**10**): 107305. DOI: 10.1088/1674-1056/ab3f98

Raman spectrum study of δ -doped GaAs/AlAs multiple-quantum wells

Wei-Min Zheng(郑卫民), Wei-Yan Cong(丛伟艳), Su-Mei Li(李素梅), Ai-Fang Wang(王爱芳), Bin Li(李斌), Hai-Bei Huang(黄海北)
Chin. Phys. B, 2018, 27 (**1**): 017302. DOI: 10.1088/1674-1056/27/1/017302

Improvement of green InGaN-based LEDs efficiency using a novel quantum well structure

Yangfeng Li(李阳锋), Yang Jiang(江洋), Junhui Die(迭俊珲), Caiwei Wang(王彩玮), Shen Yan(严珅), Ziguang Ma(马紫光), Haiyan Wu(吴海燕), Lu Wang(王禄), Haiqiang Jia(贾海强), Wenxin Wang(王文新), Hong Chen(陈弘)
Chin. Phys. B, 2017, 26 (**8**): 087311. DOI: 10.1088/1674-1056/26/8/087311

Performance improvement of InGaN/GaN multiple quantum well visible-light photodiodes by optimizing TEGa flow

Bin Li(黎斌), Shan-Jin Huang(黄善津), Hai-Long Wang(王海龙), Hua-Long Wu(吴华龙), Zhi-Sheng Wu(吴志盛), Gang Wang(王钢), Hao Jiang(江灏)
Chin. Phys. B, 2017, 26 (**8**): 087307. DOI: 10.1088/1674-1056/26/8/087307

RAPID COMMUNICATION

Lower bound on the spread of valley splitting in Si/SiGe quantum wells induced by atomic rearrangement at the interface

Gang Wang(王刚)[1,2], Shan Guan(管闪)[1], Zhi-Gang Song(宋志刚)[1], and Jun-Wei Luo(骆军委)[1,2,†]

[1] *State Key Laboratory of Superlattices and Microstructures, Institute of Semiconductors, Chinese Academy of Sciences, Beijing* 100083, *China*
[2] *Center of Materials Science and Optoelectronics Engineering, University of Chinese Academy of Sciences, Beijing* 100049, *China*

(Received 13 June 2023; revised manuscript received 5 August 2023; accepted manuscript online 21 August 2023)

The achievement of universal quantum computing critically relies on scalability. However, ensuring the necessary uniformity for scalable silicon electron spin qubits poses a significant challenge due to the considerable fluctuations in valley splitting energy (E_{VS}) across quantum dot arrays, which impede the initialization of qubit systems comprising multiple spins and give rise to spin–valley entanglement resulting in the loss of spin information. These E_{VS} fluctuations have been attributed to variations in the in-plane averaged alloy concentration along the confinement direction of Si/SiGe quantum wells. In this study, employing atomistic pseudopotential calculations, we unveil a significant spectrum of E_{VS} even in the absence of such concentration fluctuations. This spectrum represents the lower limit of the wide range of E_{VS} observed in numerous Si/SiGe quantum devices. By constructing simplified interface atomic step models, we analytically demonstrate that the lower bound of the E_{VS} spread originates from the in-plane random distribution of Si and Ge atoms within SiGe barriers — an inherent characteristic that has been previously overlooked. Additionally, we propose an interface engineering approach to mitigate the in-plane randomness-induced fluctuations in E_{VS} by inserting a few monolayers of pure Ge barrier at the Si/SiGe interface. Our findings provide valuable insights into the critical role of in-plane randomness in determining E_{VS} in Si/SiGe quantum devices and offer reliable methods to enhance the feasibility of scalable Si-based spin qubits.

Keywords: quantum wells, valley splitting, alloy concentration fluctuation

PACS: 73.21.Fg, 73.22.–f, 73.61.Cw **DOI:** 10.1088/1674-1056/acf208

1. Introduction

In the pursuit of universal fault-tolerant quantum computing, the realization of quantum error correction requires a substantial number of qubits that can be effectively controlled and coherently coupled.[1] Leveraging advanced semiconductor fabrication techniques capable of integrating billions of transistors on a single Si chip,[2] electron spins confined in Si quantum dots have emerged as a highly promising platform for quantum computing.[3] Notably, the weak intrinsic spin–orbit interaction and the presence of nuclear zero-spin isotopes contribute to a prolonged coherence time for the electron spin, effectively suppressing both spin relaxation[4,5] and dephasing.[6–8] Despite recent progress[9–16] has been made, Si spin qubits still face the challenge of valley degeneracy, which obstructs the isolation of individual two-level spin-1/2 states[9,10,14,17,18] and introduces a significant leakage channel, thereby impeding high fidelity.[5,19–22] However, the presence of discontinuous heterointerfaces, coupled with strong quantum confinement, can lift the low-lying two-fold valley degeneracy and establish an energy separation known as the valley splitting (E_{VS}). This approach effectively addresses fidelity degradation in spin-only qubits in Si. Unfortunately, the measured E_{VS} in Si/SiGe quantum wells tends to be relatively narrow, typically around tens to hundreds of μeV.[23–29] This narrow energy splitting exacerbates challenges related to rapid spin relaxation,[5,19,20] dephasing,[21,22] and errors in spin transport.[30] Moreover, the disorder in the SiGe alloy barrier introduces significant fluctuations in the valley splitting energy, ranging from nearly zero to thousands of μeV.[31–34] Consequently, this poses a significant challenge to the scalability of silicon qubits within the context of universal fault-tolerant quantum computing.[34]

Both extensive theoretical work[32,35–49] and experimental observations[24,27,28,34,50–55] have pointed out that the E_{VS} depends sensitively on the microscopic details near the interface. Particularly, a recent investigation[34] delves into the atomic-scale reconstruction of the Si/SiGe interface and reveals its three-dimensional (3D) morphology, highlighting the microscopic alloying concentration fluctuation along the confinement direction (i.e., z axis in Fig. 1(a)) as the underlying cause of the substantial spread observed in the E_{VS} measurements of various quantum dot devices. However, the in-plane randomness is inevitably ignored in their analysis since the concentration was obtained with its in-plane components averaged in advance, as illustrated in Fig. 1(b). It is worth noting that by carefully controlling the epitaxial growth of Si/SiGe heterostructures, the one-dimensional concentration fluctuation $\delta\rho_{Ge}(z)$ can be effectively minimized to a satisfactory extent, whereas the atomic random distribution within each

†Corresponding author. E-mail: jwluo@semi.ac.cn

© 2023 Chinese Physical Society and IOP Publishing Ltd

SiGe barrier layer $\rho_{\mathrm{Ge}}(x,y)$ remains uncontrollable. Therefore, the effect of in-plane randomness on E_{VS} is supposed to be more important than the out-of-plane one in terms of device preparation process. Nevertheless, the impact of this type of randomness has been largely disregarded in prior investigations,[35,37–40,43,56–60] partially due to the limitations of the adopted conventional theoretical methods.

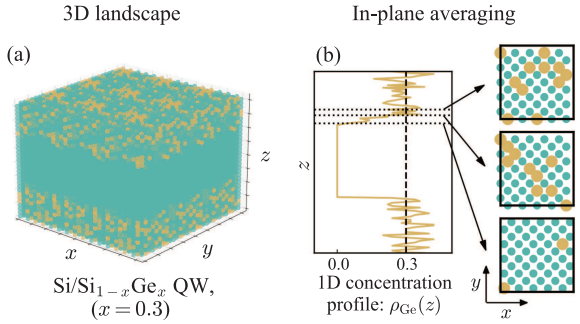


Fig. 1. (a) The three-dimensional (3D) representation showcasing the landscape of a Si/$Si_{0.7}Ge_{0.3}$ QW. (b) Schematic diagram illustrating the process of performing in-plane averaging on the concentration fluctuations of Si and Ge atoms within the 3D landscape of Si/$Si_{0.7}Ge_{0.3}$ to derive the one-dimensional (1D) concentration profiles, $\rho_{\mathrm{Ge}}(z)$.

In this study, we employ the atomistic empirical pseudopotential computation method (EPM) to investigate the impact of alloy disorder on the E_{VS} in Si/SiGe quantum well (QW). Surprisingly, we discover a remarkable and significant spread in the E_{VS}, even in the absence of alloy concentration fluctuation along the quantum confinement direction in Si/SiGe QW. Notably, we find that the minimum extent of the spread in E_{VS} is attributed to the stochastic distribution of Si and Ge atoms within the plane, independent of vertical alloy concentration fluctuations. Moreover, we elucidate the concept of in-plane random distribution of Si and Ge atoms as a consequence of changes in the interface step morphology, providing insights into the occurrence of fluctuation in the E_{VS} induced by in-plane randomness. Our results thus offer valuable guidance for enhancing the performance of Si-based spin qubits through interface engineering, highlighting the significance of addressing in-plane randomness for achieving improved qubit performance.

2. Atomistic computation method

We calculate the electronic structures of Si/SiGe QWs by directly diagonalizing the band Hamiltonian, $-\frac{1}{2}\nabla^2 + V(\boldsymbol{r})$ which is described by its potential, $V(\boldsymbol{r})$. This potential encompasses spin–orbit-coupled and nonlocal empirical pseudopotentials. For the system's pseudopotential, we employ a superposition of screened pseudopotentials $v_\alpha(r)$ of the constituent atom,[61,62]

$$V(\boldsymbol{r}) = \sum_n \sum_\alpha \hat{v}_\alpha(\boldsymbol{r} - \boldsymbol{R}_n - \boldsymbol{d}_\alpha), \tag{1}$$

where $\hat{v}_\alpha(\boldsymbol{r} - \boldsymbol{R}_n - \boldsymbol{d}_\alpha)$ represents the screened pseudopotential of atom type α at site $\boldsymbol{d}_\alpha$ in the nth primary cell, $\boldsymbol{R}_n$. The screened pseudopotential comprises a local component, $\hat{v}_\alpha^{\mathrm{loc}}(\boldsymbol{r})$, which is expressed in reciprocal space,[63] and a nonlocal spin–orbit interaction component, $\hat{v}_\alpha^{\mathrm{nonloc}}(\boldsymbol{r})$, described by the Kleinmen–Bylander formalism.[64] We diagonalize $-\frac{1}{2}\nabla^2 + V(\boldsymbol{r})$ within a plane-wave basis[61] utilizing the folded spectrum method.[65] Our approach employs a supercell combined with periodic boundary conditions. The screened pseudopotentials, $\{\hat{v}_\alpha\}$, are fitted[61] to mitigate the "LDA error" in the bulk crystal and to accurately reproduce the band gaps throughout the zone, as well as the electron and hole effective-mass tensors, valence band and conduction band offsets between well and barrier materials, spin–orbit splittings, and GW spin-splittings in bulk materials.[66] This approach has previously been applied to superlattices,[69] colloidal quantum dots,[69] and Stranski–Krastanow quantum dots.[70]

To emulate the epitaxy growth of a Si/SiGe QW on a $Si_{0.7}Ge_{0.3}$ buffer layer, where the Si QW is subject to biaxial tensile strain, we initially set the in-plane lattice constant of the supercell to the lattice constant of bulk $Si_{0.7}Ge_{0.3}$, obtained by Vegard's law. Subsequently, we determine the optimized lattice constant in the vertical direction and atomic equilibrium positions by minimizing the strain energy of the entire supercell through the use of the atomistic valence force field (VFF) method.[71,72]

3. Results and discussions

3.1. Considerable E_{VS} fluctuation in the absence of alloy concentration fluctuation

We first study the impact of alloy concentration fluctuation in the $Si_{0.7}Ge_{0.3}$ barrier on the E_{VS} of Si/$Si_{0.7}Ge_{0.3}$ QWs using EPM. To simulate the actual setups, numerous Si/$Si_{0.7}Ge_{0.3}$ QW structures are constructed through the direct sampling methods and the $Si_{0.7}Ge_{0.3}$ random alloy part comprises 3600 atoms. Each constructed Si/$Si_{0.7}Ge_{0.3}$ QWs feature distinct random alloy configurations within the $Si_{0.7}Ge_{0.3}$ barriers. Consequently, these Si/$Si_{0.7}Ge_{0.3}$ QW structures exhibit varying degrees of alloy concentration fluctuation. To quantify the extent of alloy concentration fluctuation in different Si/$Si_{0.7}Ge_{0.3}$ QW structures, we utilize $\sigma(\rho_{\mathrm{Ge}}(z))$ as a measure, as defined in the caption of Fig. 2. As illustrated in Figs. 2(a)–2(b), the representative Ge concentration profiles clearly show the reduction in size of the alloy concentration fluctuation within the Si/$Si_{0.7}Ge_{0.3}$ QW. Notably, it is challenging to precisely control the magnitude of alloy concentration fluctuation to achieve sufficiently small values through random sampling of the $Si_{0.7}Ge_{0.3}$ barrier. To address this issue, we build $Si_{0.7}Ge_{0.3}$ by spatially restricting the degrees of freedom of the random configuration space. Specifically, we

systematically produce a set of Si/$Si_{0.7}Ge_{0.3}$ QWs by maintaining a constant Si-to-Ge atom ratio per atomic monolayer (ML) along the vertical direction. Meanwhile, the distribution of Si and Ge atoms is randomized within each barrier layer. In this way, we obtain the concentration profile of ideal laterally infinite Si/$Si_{0.7}Ge_{0.3}$ QW (see Fig. 2(c)).

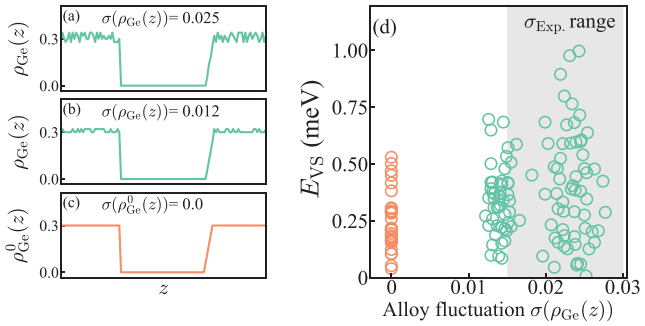


Fig. 2. (a)–(c) In-plane averaged Ge concentration distributions of Si/$Si_{0.7}Ge_{0.3}$ QWs. Panel (c) corresponds to the ideal laterally infinite Si/$Si_{0.7}Ge_{0.3}$ QW, with its Ge concentration function denoted by $\rho^0_{Ge}(z)$. The magnitude of the alloy concentration fluctuation in Si/$Si_{0.7}Ge_{0.3}$ QWs is quantified through $\sigma(\rho_{Ge}(z)) = \sqrt{\frac{1}{l_b}\int dz\left[\rho_{Ge}(z) - \rho^0_{Ge}(z)\right]^2}$, where l_b is the length of $Si_{0.7}Ge_{0.3}$ barrier. From (a) to (c), Si/$Si_{0.7}Ge_{0.3}$ QW has decreased degree of alloy concentration fluctuation and with vanished fluctuation magnitude in (c). (d) The valley splittings in Si/$Si_{0.7}Ge_{0.3}$ QWs (with 10 MV/m of electric field applied in the QW confinement direction), calculated using the atomistic empirical pseudopotential method, are presented as a function of the magnitude of alloy concentration fluctuations within the $Si_{0.7}Ge_{0.3}$ barrier. The scattered data points represent Si/$Si_{0.7}Ge_{0.3}$ QWs with diverse random alloy configurations. The green empty circles correspond to Si/$Si_{0.7}Ge_{0.3}$ QWs with a finite size of alloy concentration fluctuation in the $Si_{0.7}Ge_{0.3}$ barrier. The orange empty circles correspond to ideal laterally infinite Si/$Si_{0.7}Ge_{0.3}$ QWs without any alloy concentration fluctuation in the $Si_{0.7}Ge_{0.3}$ barrier. The shaded region represents the experimentally observed range of alloy concentration fluctuations. The energy fluctuation in the valley splitting, in the absence of alloy concentration fluctuation, is indicated as $\delta E_{VS} = 3 \times \sigma(E_{VS})$ (three-sigma control limit are used to quantify the energy spread of valley splitting).

Upon obtaining a range of Si/$Si_{0.7}Ge_{0.3}$ QW structures with varying degrees of alloy concentration fluctuation, we then carry out calculation to determine the corresponding E_{VS}. Within the atomistic simulation, a 10 MV/m of electric field is applied in the QW confinement direction. There are two reasons for applying an electric field: First, in real SiGe quantum devices, there is typically a perpendicular electric field across the SiGe heterostructure in the order of a few MV/m. Second, it is well studied that the valley splitting in Si/SiGe quantum wells fast decays with an increasing thickness of the quantum well and exhibits oscillations at the atomic scale ($\sim$ 3 ML).[37,38,40,58] To ensure a focused investigation on the electronic states near the interface of one side of the quantum well and avoid the influence of the interface on the other side, an electric field is applied in the z-direction which confines the electronic states to the desired region of interest. However, the presence of an electric field can exacerbate the effect of potential variation resulting from SiGe disorder on the electronic states within the Si quantum well. Specifically, a higher electric field strength can lead to more pronounced fluctuations in the valley splitting in Si/SiGe quantum wells. From Fig. 2(d), one observes that an increased degree of alloy concentration fluctuation within the Si/$Si_{0.7}Ge_{0.3}$ QW leads to a greater energy fluctuation of E_{VS}, as denoted by the green empty circles in Fig. 2(d). Moreover, increasing the degree of alloy concentration fluctuation generally increases the E_{VS}. These findings align with the conclusions drawn in Ref. [34], indicating that alloy concentration fluctuation along z is responsible for the spreading of the energy fluctuation in E_{VS}. However, our atomistic calculations (depicted by the orange empty circles in Fig. 2(d)) show that, even in the absence of alloy concentration fluctuation within the Si/$Si_{0.7}Ge_{0.3}$ QW, a substantial energy fluctuation in E_{VS}, amounting to $\pm$0.33 meV, persists. This significant fluctuation arises solely from the random in-plane distribution of Si and Ge atoms within the $Si_{0.7}Ge_{0.3}$ barrier layer. Remarkably, this fluctuation in E_{VS} is comparable in magnitude to the one caused by the alloy concentration fluctuation. It is crucial to emphasize that while the concentration fluctuation of the $Si_{0.7}Ge_{0.3}$ barrier in the vertical direction can be mitigated through the epitaxial growth of Si/$Si_{0.7}Ge_{0.3}$ heterostructures with low-temperature budget, the atomic random distribution within the SiGe barrier layer remains uncontrollable. Consequently, such a uncertain E_{VS} resulting from the in-plane atomic randomness is an inherent characteristic and represents the lower bound of the energy fluctuation in Si/$Si_{0.7}Ge_{0.3}$ QWs.

It should be clarified that, in the process of generating SiGe random alloys, we deliberately opted for a finite supercell size, a choice that unavoidably introduces some hypothetical order within the SiGe alloys. Nevertheless, we wish to reiterate our stance that our study is primarily centered on the comparative evaluation of the energy ranges associated with E_{VS} variations within the two distinct Si/SiGe QW structural categories ($\sigma(\rho_{Ge}(z)) \neq 0$ and $\sigma(\rho_{Ge}(z)) = 0$). The utilization of a finite supercell size inherently contributes to an augmentation of the E_{VS} fluctuation in both classes of Si/SiGe QW structures. However, it is noteworthy that the inherent characteristics of the supercell size exert minimal influence on the relative magnitudes of these energy ranges. Our focus remains directed toward discerning the relative size of E_{VS} fluctuation between the two aforementioned structural categories.

3.2. Effect of interface atomic step on E_{VS}

Having identified the lower bound of the E_{VS} spread in Si/$Si_{0.7}Ge_{0.3}$ QWs, we next clarify its origin by using a simplified atomic step model. Since E_{VS} is recognized as an interface-related phenomenon, the in-plane atomic randomness effect within the barrier alloying layer predominantly relies on the behavior of interface roughness. This behavior can be basically described by a sequence of atomic step edges at the interfaces, as depicted in Figs. 3(a)–3(b). To streamline the

discussion and focus on the impact of a single interface atomic step edge on $E_{\rm VS}$, we deliberately select pure Ge as the barrier material for the Si QWs, instead of $Si_{0.7}Ge_{0.3}$. By doing so, we isolate the influence of alloy disorder and direct our attention specifically toward the interface step effect.

We consider a scenario where a one-monolayer-tall ($a/4$) interface atomic step edge, along the y-direction, is positioned at $x = \gamma L_x$ (where a is the Si lattice constant and L_x represents the supercell size in the x-direction), as depicted in Fig. 3(c). The calculated $E_{\rm VS}$ dependent on the step position is plotted in Fig. 3(d). Notably, one observes a significant alteration in the $E_{\rm VS}$ when the interface step is moved along the x direction, with the magnitude of $E_{\rm VS}$ reaching its minimum when the interface step is located at $0.4L_x$.

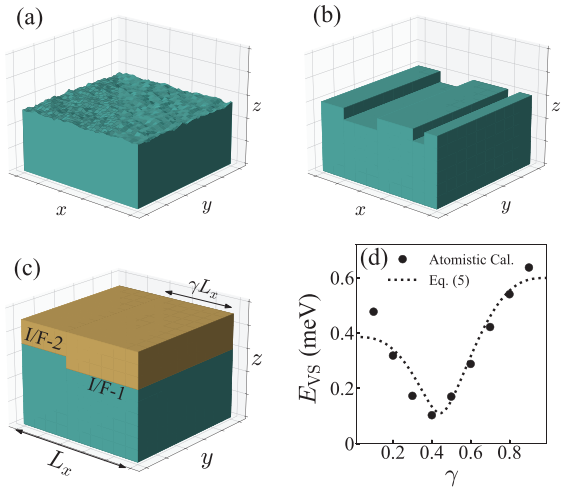


Fig. 3. (a) Schematic diagram of interface roughness. (b) Diagrammatic drawing of interface atomic step edges. (c) Illustration depicting the schematic representation of the top interface of the Si/Ge QW, where a one ML-tall atomic step is present. (d) The valley splitting in Si/Ge QW is examined by varying the position of a single atomic step within the interface plane. The height of the atomic step is precisely one ML or $a/4$. An electric field of 9 MV/m is applied to drive the electrons toward the QW interface with the atomic steps. The results obtained from atomistic calculations are denoted by black dots, while the numerical outcomes derived from Eq. (5) are represented by the dotted line. The fitted parameters of Eq. (5) are determined to be $\alpha/\beta = 1.55$ and $\omega = 0.10\pi$.

To elucidate the suppressive effect of the interface step on $E_{\rm VS}$, we establish an effective mass model. The interface atomic step depicted in Fig. 3(c) can be conceptualized as dividing one interface (at $z_{\rm I/F}$) into two halves and vertically shifting one half upward by one ML ($a/4$). This process gives rise to two laterally distributed half-interfaces, labeled as I/F-1 and I/F-2. When an external electric field F is applied along the QW growth (z) direction, the electronic states primarily localize at the upper interface containing the atomic step. The corresponding confinement potential can be expressed as[47,48]

$$\begin{aligned} U(r) =& \underbrace{U_0\Theta(z-z_{\rm I/F-1})\,\mathrm{rect}\left(\frac{x-\gamma L_x/2}{\gamma L_x}\right)}_{\rm I/F-1} \\ &+ \underbrace{U_0\Theta(z-z_{\rm I/F-2})\,\mathrm{rect}\left(\frac{x-(1+\gamma)L_x/2}{(1-\gamma)L_x}\right)}_{\rm I/F-2} \\ &- eFz/\varepsilon, \end{aligned} \tag{2}$$

here ε denotes the dielectric constant and $\mathrm{rect}(x)$ represents the rectangle function.[73] The vertical coordinates of the two laterally distributed single interfaces are related by $z_{\rm I/F-2} = z_{\rm I/F-1} + \frac{a}{4}$. For a single interface (I/F) located at $z_{\rm I/F}$, the valley coupling matrix can be expressed using the effective mass approximation theory[40,48,60] as follows:

$$\begin{aligned} H^{\rm I/F}_{\Delta_{+z},\Delta_{-z}} &= \langle \Delta_{+z}|U(r)|\Delta_{-z}\rangle \\ &= \frac{\Sigma U_0}{2ik_0}\left|f(z_{\rm I/F})\right|^2 \mathrm{e}^{-2ik_0 z_{\rm I/F}}. \end{aligned} \tag{3}$$

Here, $\left|f(z_{\rm I/F})\right|$ represents the envelope function at the interface, and $k_0 = 0.85\times\frac{2\pi}{a}$ is the position of the conduction band minimum in the FCC Brillouin zone. Equation (3) encompasses the summation of plane wave coefficients (Σ) and incorporates the conduction band offset U_0 between the Si well and Ge barrier. The electric field has a negligible impact on the valley coupling (see Appendix A for a detailed derivation). Consequently, we can approximate the valley coupling induced by an interface step as a linear combination of two laterally distributed single interfaces,

$$\begin{aligned} H^{\rm s\text{-}I/S}_{\Delta_{+z},\Delta_{-z}} &= \langle \Delta_{+z}|U(r)|\Delta_{-z}\rangle \approx H^{\rm I/F\text{-}1}_{\Delta_{+z},\Delta_{-z}} + H^{\rm I/F\text{-}2}_{\Delta_{+z},\Delta_{-z}} \\ &= \frac{\Sigma U_0}{2ik_0}\left|f\left(z_{\rm I/F-1}\right)\right|^2 \mathrm{e}^{-i2k_0 z_{\rm I/F-1}}\left(\gamma - \frac{\sin(2\pi\gamma)}{2\pi}\right) \\ &\quad + \frac{\Sigma U_0}{2ik_0}\left|f\left(z_{\rm I/F-2}\right)\right|^2 \mathrm{e}^{-i2k_0 z_{\rm I/F-2}} \\ &\quad \times\left(1-\gamma+\frac{\sin(2\pi\gamma)}{2\pi}\right). \end{aligned} \tag{4}$$

In the approximation, we have assumed the in-plane wave function as $\sqrt{\frac{2}{L_x}}\sin(\frac{\pi}{L_x}\cdot x)$, representing an electron in a box. We label the valley coupling matrix due to a single interface step as "s-I/S". The distinction between $\left|f(z_{\rm I/F-1})\right|^2$ and $\left|f\left(z_{\rm I/F-2}\right)\right|^2$ is parameterized as α and β. Therefore, the determination of $E_{\rm VS}$ in the presence of an atomic step can be obtained as

$$\begin{aligned} E_{\rm VS} &= 2\left|H^{\rm s\text{-}I/S}_{\Delta_{+z},\Delta_{-z}}\right| \\ &= C\left|\mathrm{e}^{i\omega}\left[\alpha\left(\gamma-\frac{\sin(2\pi\gamma)}{2\pi}\right)\right.\right. \\ &\quad \left.\left.+\beta\,\mathrm{e}^{-ik_0 a/2}\left(1-\gamma+\frac{\sin(2\pi\gamma)}{2\pi}\right)\right]\right|, \end{aligned} \tag{5}$$

where $\mathrm{e}^{i\omega}$ represents an extra phase change induced by the valley coupling.[38] To validate the effective model developed above, we perform a fitting procedure using our atomistic calculation results of $E_{\rm VS}$ and Eq. (5), with adjustments made to

the parameters C, ω, and α/β. The results, as depicted in Fig. 3(d), demonstrate the capability of the model, incorporating two laterally distributed interfaces, to accurately describe the impact of the interface atomic step on $E_{\rm VS}$. The effective model reveals that the atomic-step-position-dependent behavior of $E_{\rm VS}$ arises from a phase difference $e^{-ik_0a/2}$ between the two laterally distributed interfaces, which are vertically separated by one ML.

3.3. Effect of in-plane random distribution of Si, Ge atoms on $E_{\rm VS}$

The effective model can be easily extended to investigate scenarios involving multiple interface atomic steps, which contain the changes in the surface topography and can largely reflect the in-plane random distribution of Si and Ge atoms in the absence of alloy concentration fluctuations along the quantum confinement axis. To explore the effects of multiple interface atomic steps on $E_{\rm VS}$, we initially consider the case of a single interface step positioned at γL_x, where the Ge concentration in the nearest neighboring SiGe atomic layer to the Si QW is γ. In order to approximate the random distribution of Si and Ge atoms within the SiGe layer while maintaining a constant Ge concentration, we divide the entire width of the in-plane Ge section, observed in the case of a single step, into two sections separated by a distance of λL_x, as depicted in Fig. 4(a). This separation generates four interface segments, each characterized by its vertical coordinate $z_{{\rm I/F}-i}$, center position x_i and width w_i along the x direction. As a result, the QW potential takes on a specific form denoted as

$$U(r)=\sum_{i=1}^{4}U_0\Theta(z-z_{{\rm I/F}-i}){\rm rect}\left(\frac{x-x_i}{w_i}\right), \tag{6}$$

where the vertical coordinates follow the relationship $z_{\rm I/F-2}=z_{\rm I/F-4}=z_{\rm I/F-1}+\frac{a}{4}=z_{\rm I/F-3}+\frac{a}{4}$. The center positions are determined as $x_1=\gamma L_x/4$, $x_2=(\gamma L_x+\lambda L_x)/2$, $x_3=(\frac{3}{2}\gamma L_x+2\lambda L_x)/2$, and $x_4=(\gamma L_x+\lambda L_x+L_x)/2$. The widths are given by $w_1=w_3=\gamma L_x/2$, $w_2=\lambda L_x$, and $w_4=L_x-\sum_{i=1}^{3}w_i$. Similar to the methodology used for a single interface step, we can apply a superposition method to estimate the valley coupling resulting from multiple interface steps (m-I/S). By considering four laterally distributed single interfaces as contributing factors, we obtain the following equation:

$$H^{\rm m\text{-}I/S}_{\Delta_{+z},\Delta_{-z}}=\langle\Delta_{+z}|U(r)|\Delta_{-z}\rangle\approx\sum_{i=1}^{4}H^{{\rm I/F}-i}_{\Delta_{+z},\Delta_{-z}}. \tag{7}$$

Having determined the parameters C, ω, and α/β in Eq. (5) through fitting the results of atomistic simulations, we can readily compute the $E_{\rm VS}$ for multiple interface steps using the derived equation

$$\begin{aligned}E_{\rm VS}&=2\left|H^{\rm m\text{-}I/S}_{\Delta_{+z},\Delta_{-z}}\right|\\&=C\Big|e^{i\omega}\Big[\alpha\left(\frac{\gamma}{2}-\frac{\sin(\pi\gamma)}{2\pi}\right)+\beta e^{-ik_0a/2}\\&\quad\times\left(\lambda+\frac{\sin(\pi\gamma)}{2\pi}-\frac{\sin[\pi(\gamma+2\lambda)]}{2\pi}\right)\\&\quad+\alpha\left(\frac{\gamma}{2}-\frac{\sin[2\pi(\gamma+\lambda)]}{2\pi}+\frac{\sin[\pi(\gamma+2\lambda)]}{2\pi}\right)\\&\quad+\beta e^{-ik_0a/2}\left(1-\gamma-\lambda+\frac{\sin[2\pi(\gamma+\lambda)]}{2\pi}\right)\Big]\Big|.\end{aligned} \tag{8}$$

Figure 4(b) represents the dependence of $E_{\rm VS}$ on two factors: the fractional width of the in-plane Ge section before the step separation, denoted as γ, and the fractional distance of the step separation, denoted as λ. It is evident that, for a fixed γ corresponding to the intra-layer Ge concentration, varying the separation distances λ leads to distinct values of $E_{\rm VS}$. This observation underscores how the rearrangement of Si and Ge atoms within a 1 ML-thick interface layer can induce changes in $E_{\rm VS}$.

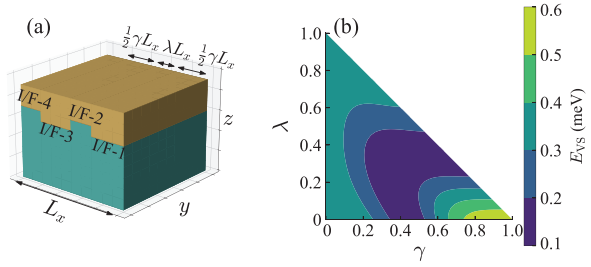


Fig. 4. (a) A schematic diagram illustrating the separation of interface atomic steps. The initial in-plane Ge section with a width of γL_x is equally divided into two subsections, which are separated by a distance of λL_x. (b) The valley splitting energy is calculated using the step separation model, represented by Eq. (8). The parameters C, ω, and α/β in Eq. (8) (multiple steps) are consistent with those in Eq. (5) (single step). The variation of $E_{\rm VS}$ is shown as a function of the fractional width of the in-plane Ge section before the step separation, denoted as γ, and the fractional separation spacing, denoted as λ. The values of γ and λ adhere to the constraint $\gamma+\lambda<1$.

3.4. Eliminating the $E_{\rm VS}$ fluctuation caused by in-plane random distribution of Si, Ge atoms

Based on the preceding discussions, it is evident that the fluctuation of valley splitting induced by in-plane randomness imposes a lower limit on the wide spectrum of $E_{\rm VS}$ in $Si/Si_{0.7}Ge_{0.3}$ QWs, presenting a challenge to the integration of Si electron spin qubits. To tackle this issue, we explore strategies to mitigate this lower limit through interface engineering. Our proposed approach involves the epitaxial growth of a thin Ge layer before the heterogeneous growth of $Si_{0.7}Ge_{0.3}$ on the Si active layer. The inclusion of a thin Ge layer at the $Si/Si_{0.7}Ge_{0.3}$ interface effectively separates the Si well and SiGe barrier, ensuring that the wave function of $\Delta_{\pm z}$ valley states remains immune to in-plane potential fluctuations arising from the disorder in the distribution of Si and Ge atoms within the $Si_{0.7}Ge_{0.3}$ barrier layer, as depicted in Figs. 5(a)–5(b). Consequently, both the valley coupling and valley splitting in the Si active layer remain unaffected by the disorder within the $Si_{0.7}Ge_{0.3}$ barrier. We substantiate this proposition

through atomistic EPM simulations, as illustrated in Fig. 5(c). These simulations demonstrate an exponential reduction in the fluctuation of $E_{\rm VS}$ resulting from the random distribution of Si and Ge atoms within the $Si_{0.7}Ge_{0.3}$ barrier layer as the thickness of the interfacial Ge layer increases. Remarkably, the introduction of a 4-ML thick interfacial Ge layer diminishes the fluctuation in $E_{\rm VS}$ to one-tenth of its original magnitude. It is worth emphasizing that our prior calculations[33,74] have shown a significant amplification of $E_{\rm VS}$ with the incorporation of a 4-ML thick Ge layer at the Si QW interface, and this result has also been experimentally validated.[75]

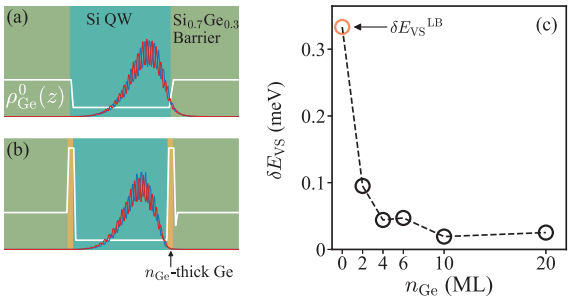


Fig. 5. (a) Schematic diagram illustrating the structure of the $Si/Si_{0.7}Ge_{0.3}$ QW is presented, where the white solid line represents the distribution of Ge concentration, while the red and blue solid lines depict the wave functions of the split $\Delta_{\pm z}$ valley states. (b) Schematic diagram showcasing the structure of the $Si/n_{\rm Ge}$-thick $Ge/Si_{0.7}Ge_{0.3}$ QW is displayed, with emphasis on the Ge concentration profile and the wave function of the split $\Delta_{\pm z}$ valley states. (c) The energy fluctuation of valley splitting, resulting from the in-plane random distribution of Si and Ge atoms near the $Si/Si_{0.7}Ge_{0.3}$ interface in the $Si_{0.7}Ge_{0.3}$ barrier, is effectively mitigated through the insertion of a few Ge layers at the interface. The magnitude of $E_{\rm VS}$ fluctuation, quantified by $\delta E_{\rm VS}$, is plotted on the vertical axis, while the thickness of the inserted Ge layer in monolayers (ML) is shown on the horizontal axis. $\delta E_{\rm VS}{}^{\rm LB}$ at $n_{\rm Ge}=0$ ML is the lower bound of $E_{\rm VS}$ fluctuation in $Si/Si_{0.7}Ge_{0.3}$ QWs, labeled with superscript "LB".

4. Conclusions

Our investigation has provided significant insights into the phenomenon of $E_{\rm VS}$ in Si/SiGe QWs. Surprisingly, we have demonstrated that a substantial spread of $E_{\rm VS}$ can occur even in the absence of concentration fluctuation. This spread, which arises solely from the in-plane random distribution of Si and Ge atoms within the SiGe barrier, represents the lower bound of the wide spectrum of $E_{\rm VS}$ observed in various Si/SiGe devices. We have developed effective atomic step models to describe the impact of in-plane disorder on $E_{\rm VS}$. By recognizing and incorporating the influence of in-plane randomness, we propose an experimentally feasible method to mitigate the fluctuation of $E_{\rm VS}$ through the design of the interface atomic structure. Specifically, we suggest the inclusion of a thin Ge layer at the Si/SiGe interface, which effectively reduces the alloying-disorder-induced $E_{\rm VS}$ fluctuations. Our study thus paves the way for the development of more reliable Si-based electron spin qubits.

Appendix A: Local interface induced valley coupling

With the allowed valley coupling, we now calculate the matrix element $H^{\rm I/F}_{\Delta_{+z},\Delta_{-z}}=\langle\Delta_{+z}|U(r)|\Delta_{-z}\rangle$. We consider the perturbation Hamiltonian as a local sharp interface with an electric field, $U(r)=U_0\Theta(z-z_{\rm I})-e\frac{F}{\varepsilon}z$, where U_0 is the barrier height, and $z_{\rm I}$ is the interface position. Thus the valley coupling matrix is given by

$$\begin{aligned}H^{\rm I/F}_{\Delta_{+z},\Delta_{-z}}&=\langle\Delta_{+z}|U(z)|\Delta_{-z}\rangle+H^{eF/\varepsilon}_{\Delta_{+z},\Delta_{-z}}\\&=\int\int\int {\rm d}x{\rm d}y{\rm d}z u^*_+ u_- {\rm e}^{-{\rm i}2k_0z}|f(z)|^2U_0\Theta(z-z_{\rm I})+H^{eF/\varepsilon}_{\Delta_{+z},\Delta_{-z}}\\&=\Sigma U_0\int {\rm d}z{\rm e}^{-{\rm i}2k_0z}|f(z)|^2\Theta(z-z_{\rm I})+H^{eF/\varepsilon}_{\Delta_{+z},\Delta_{-z}},\end{aligned}\tag{A1}$$

where the periodic Bloch waves are expanded as plane waves $u_\pm(r)=\sum_{\boldsymbol{G}}C_\pm(\boldsymbol{G}){\rm e}^{-{\rm i}\boldsymbol{G}\cdot\boldsymbol{r}}$, and Σ denotes the summation of coefficients of plane waves $\Sigma=\sum_{\boldsymbol{G}}C^*_+(\boldsymbol{G})C_-(\boldsymbol{G})$, here only $\boldsymbol{G}_1=\boldsymbol{G}_2$ case is considered since $\boldsymbol{G}_1\neq\boldsymbol{G}_2$ terms would lead to fast oscillations in the integrand that average to zero. In Eq. (A1) we integrate by parts the first term

$$\begin{aligned}H^{\rm I/F}_{\Delta_{+z},\Delta_{-z}}&=\frac{\Sigma U_0}{-{\rm i}2k_0}\int|f(z)|^2\Theta(z-z_{\rm I/F}){\rm d}\,{\rm e}^{-{\rm i}2k_0z}+H^{eF/\varepsilon}_{\Delta_{+z},\Delta_{-z}}\\&=\frac{\Sigma U_0}{-{\rm i}2k_0}|f(z)|^2\Theta(z-z_{\rm I/F}){\rm e}^{-{\rm i}2k_0z}|^{+\infty}_{-\infty}+\frac{\Sigma U_0}{{\rm i}2k_0}\int{\rm d}\left(|f(z)|^2\Theta(z-z_{\rm I/F})\right){\rm e}^{-{\rm i}2k_0z}+H^{eF/\varepsilon}_{\Delta_{+z},\Delta_{-z}}\\&=\frac{\Sigma U_0}{{\rm i}2k_0}\int{\rm e}^{-{\rm i}2k_0z}|f(z)|^2\delta(z-z_{\rm I}){\rm d}z+\frac{\Sigma U_0}{{\rm i}2k_0}\int{\rm e}^{-{\rm i}2k_0z}\Theta(z-z_{\rm I/F})\frac{{\rm d}\,|f(z)|^2}{{\rm d}z}{\rm d}z+H^{eF/\varepsilon}_{\Delta_{+z},\Delta_{-z}}\\&=\underbrace{\frac{\Sigma U_0}{{\rm i}2k_0}{\rm e}^{-{\rm i}2k_0z_{\rm I/F}}\left|f(z_{\rm I/F})\right|^2}_{H^{\rm I/F(0)}_{\Delta_{+z},\Delta_{-z}}}+\underbrace{\frac{\Sigma U_0}{{\rm i}2k_0}\int{\rm e}^{-{\rm i}2k_0z}\Theta(z-z_{\rm I/F})\frac{{\rm d}\,|f(z)|^2}{{\rm d}z}{\rm d}z+H^{eF/\varepsilon}_{\Delta_{+z},\Delta_{-z}}}_{H^{\rm I/F(1)}_{\Delta_{+z},\Delta_{-z}}}.\end{aligned}\tag{A2}$$

Equation (A2) shows that the valley coupling can be divided into the zero-order and the first-order terms: they correspond to the value of the envelope function at the interface and the tunneling into the barrier, respectively. We evaluate their contributions to $H^{\mathrm{I/F}}_{\Delta_{+z},\Delta_{-z}}$ respectively in Fig. A1. The numerical results demonstrate that $H^{\mathrm{I/F(0)}}_{\Delta_{+z},\Delta_{-z}}$ is a good approximation to $H^{\mathrm{I/F}}_{\Delta_{+z},\Delta_{-z}}$ since the $\left|H^{\mathrm{I/F(0)}}_{\Delta_{+z},\Delta_{-z}}\right|$ magnitude is way larger than $\left|H^{\mathrm{I/F(1)}}_{\Delta_{+z},\Delta_{-z}}\right|$ in case of weak field. This approximation was also approved in Refs. [59,60]. As a result, we can obtain the local C_{2v} symmetry induced valley coupling,

$$H^{\mathrm{I/F}}_{\Delta_{+z},\Delta_{-z}} \approx H^{\mathrm{I/F(0)}}_{\Delta_{+z},\Delta_{-z}}(z_{\mathrm{I/F}}) = \frac{\Sigma U_0}{\mathrm{i}2k_0}\left|f(z_{\mathrm{I/F}})\right|^2 \mathrm{e}^{-\mathrm{i}2k_0 z_{\mathrm{I/F}}}. \quad \text{(A3)}$$

The E_{VS} is given by $E_{\mathrm{VS}} = 2\left|H^{\mathrm{I/F}}_{\Delta_{+z},\Delta_{-z}}\right|$. Equation (A3) shows that valley coupling arising from the local C_{2v} symmetry is a complex number. Its modulus is proportional to the barrier height U_0 and the envelope function $\left|f(z_{\mathrm{I/F}})\right|^2$ at the interface. Its phase is determined by the interface position in the direction of the QW confinement. The similar expression for the valley coupling matrix has been obtained before.[40,59,60]

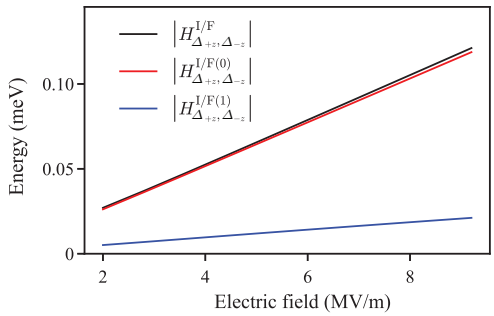


Fig. A1. The contribution of each term in Eq. (A2). The thickness of Si/Ge QW is 10 nm. The barrier height is 150 meV. For the summation of the plane expansion coefficients of Bloch waves, $\Sigma = -0.2607$.[48,60]

Acknowledgements

Project supported by the National Science Fund for Distinguished Young Scholars (Grant No. 11925407), the Basic Science Center Program of the National Natural Science Foundation of China (Grant No. 61888102), and the Key Research Program of Frontier Sciences of CAS (Grant No. ZDBS-LY-JSC019), and CAS Project for Young Scientists in Basic Research (Grant No. YSBR-026).

References

[1] DiVincenzo D P 2000 *Fortschritte der Physik* **48** 771
[2] Vandersypen L M K and Eriksson M A 2019 *Physics Today* **72** 38
[3] Loss D and DiVincenzo D P 1998 *Phys. Rev. A* **57** 120
[4] Morello A, Pla J J, Zwanenburg F A, Chan K W, Tan K Y, Huebl H, Möttönen M, Nugroho C D, Yang C, van Donkelaar J A, Alves A D C, Jamieson D N, Escott C C, Hollenberg L C L, Clark R G and Dzurak A S 2010 *Nature* **467** 687
[5] Yang C H, Rossi A, Ruskov R, Lai N S, Mohiyaddin F A, Lee S, Tahan C, Klimeck G, Morello A and Dzurak A S 2013 *Nat. Commun.* **4** 2069
[6] Assali L V C, Petrilli H M, Capaz R B, Koiller B, Hu X and Das Sarma S 2011 *Phys. Rev. B* **83** 165301
[7] Tyryshkin A M, Tojo S, Morton J J L, Riemann H, Abrosimov N V, Becker P, Pohl H J, Schenkel T, Thewalt M L W, Itoh K M and Lyon S A 2012 *Nat. Mater.* **11** 143
[8] Steger M, Saeedi K, Thewalt M L W, Morton J J L, Riemann H, Abrosimov N V, Becker P and Pohl H J 2012 *Science* **336** 1280
[9] Yang C H, Leon R C C, Hwang J C C, Saraiva A, Tanttu T, Huang W, Camirand Lemyre J, Chan K W, Tan K Y, Hudson F E, Itoh K M, Morello A, Pioro-Ladrière M, Laucht A and Dzurak A S 2020 *Nature* **580** 350
[10] Petit L, Eenink H G J, 314 Russ M, Lawrie W I L, Hendrickx N W, Philips S G J, Clarke J S, Vandersypen L M K and Veldhorst M 2020 *Nature* **580** 355
[11] Yoneda J, Takeda K, Otsuka T, Nakajima T, Delbecq M R, Allison G, Honda T, Kodera T, Oda S, Hoshi Y, Usami N, Itoh K M and Tarucha S 2018 *Nat. Nanotechnol.* **13** 102
[12] Yang C H, Chan K W, Harper R, Huang W, Evans T, Hwang J C C, Hensen B, Laucht A, Tanttu T, Hudson F E, Flammia S T, Itoh K M, Morello A, Bartlett S D and Dzurak A S 2019 *Nat. Electron.* **2** 151
[13] Veldhorst M, Yang C H, Hwang J C C, Huang W, Dehollain J P, Muhonen J T, Simmons S, Laucht A, Hudson F E, Itoh K M, Morello A and Dzurak A S 2015 *Nature* **526** 410
[14] Watson T F, Philips S G J, Kawakami E, Ward D R, Scarlino P, Veldhorst M, Savage D E, Lagally M G, Friesen M, Coppersmith S N, Eriksson M A and Vandersypen L M K 2018 *Nature* **555** 633
[15] Sigillito A J, Gullans M J, Edge L F, Borselli M and Petta J R 2019 *npj Quantum Inf.* **5** 1
[16] Chan K W, Sahasrabudhe H, Huang W, Wang Y, Yang H C, Veldhorst M, Hwang J C C, Mohiyaddin F A, Hudson F E, Itoh K M, Saraiva A, Morello A, Laucht A, Rahman R and Dzurak A S 2021 *Nano Lett.* **21** 1517
[17] Maurand R, Jehl X, Kotekar-Patil D, Corna A, Bohuslavskyi H, Laviéville R, Hutin L, Barraud S, Vinet M, Sanquer M and De Franceschi S 2016 *Nat. Commun.* **7** 13575
[18] Huang W, Yang C H, Chan K W, Tanttu T, Hensen B, Leon R C C, Fogarty M A, Hwang J C C, Hudson F E, Itoh K M, Morello A, Laucht A and Dzurak A S 2019 *Nature* **569** 532
[19] Tahan C and Joynt R 2014 *Phys. Rev. B* **89** 075302
[20] Huang P and Hu X 2014 *Phys. Rev. B* **90** 235315
[21] Hu X 2011 *Phys. Rev. B* **83** 165322
[22] Gamble J K, Friesen M, Coppersmith S N and Hu X 2012 *Phys. Rev. B* **86** 035302
[23] Zajac D M, Hazard T M, Mi X, Wang K and Petta J R 2015 *Appl. Phys. Lett.* **106** 223507
[24] Goswami S, Slinker K A, Friesen M, McGuire L M, Truitt J L, Tahan C, Klein L J, Chu J O, Mooney P M, van der Weide D W, Joynt R, Coppersmith S N and Eriksson M A 2006 *Nat. Phys.* **3** 41
[25] Wuetz B P, Losert M P, Tosato A, Lodari M, Bavdaz P L, Stehouwer L, Amin P, Clarke J S, Coppersmith S N, Sammak A, Veldhorst M, Friesen M and Scappucci G 2020 *Phys. Rev. Lett.* **125** 186801
[26] Mi X, Péterfalvi C G, Burkard G and Petta J 2017 *Phys. Rev. Lett.* **119** 176803
[27] Hollmann A, Struck T, Langrock V, Schmidbauer A, Schauer F, Leonhardt T, Sawano K, Riemann H, Abrosimov N V, Bougeard D and Schreiber L R 2020 *Phys. Rev. Appl.* **13** 034068
[28] Borselli M G, Ross R S, Kiselev A A, Croke E T, Holabird K S, Deelman P W, Warren L D, Alvarado-Rodriguez I, Milosavljevic I, Ku F C, Wong W S, Schmitz A E, Sokolich M, Gyure M F and Hunter A T 2011 *Appl. Phys. Lett.* **98** 123118
[29] Borjans F, Zajac D, Hazard T and Petta J 2019 *Phys. Rev. Appl.* **11** 044063
[30] Zhao X and Hu X 2019 arXiv:1803.00749 [cond-mat, physics:quant-ph]
[31] Srinivasan S, Klimeck G and Rokhinson L P 2008 *Appl. Phys. Lett.* **93** 112102
[32] Jiang Z, Kharche N, Boykin T and Klimeck G 2012 *Appl. Phys. Lett.* **100** 103502
[33] Zhang L, Luo J W, Saraiva A, Koiller B and Zunger A 2013 *Nat. Commun.* **4** 2396

[34] Paquelet Wuetz B, Losert M P, Koelling S, Stehouwer L E A, Zwerver A M J, Philips S G J, Madzik M T, Xue X, Zheng G, Lodari M, Amitonov S V, Samkharadze N, Sammak A, Vandersypen L M K, Rahman R, Coppersmith S N, Moutanabbir O, Friesen M and Scappucci G 2022 *Nat. Commun.* **13** 7730

[35] Sham L J and Nakayama M 1979 *Phys. Rev. B* **20** 734

[36] Ando T 1979 *Phys. Rev. B* **19** 3089

[37] Boykin T B, Klimeck G, Friesen M, Coppersmith S N, von Allmen P, Oyafuso F and Lee S 2004 *Phys. Rev. B* **70** 165325

[38] Nestoklon M O, Golub L E and Ivchenko E L 2006 *Phys. Rev. B* **73** 235334

[39] Friesen M, Eriksson M A and Coppersmith S N 2006 *Appl. Phys. Lett.* **89** 202106

[40] Friesen M, Chutia S, Tahan C and Coppersmith S N 2007 *Phys. Rev. B* **75** 115318

[41] Kharche N, Prada M, Boykin T B and Klimeck G 2007 *Appl. Phys. Lett.* **90** 092109

[42] Friesen M and Coppersmith S N 2010 *Phys. Rev. B* **81** 115324

[43] Culcer D, Hu X and Das Sarma S 2010 *Phys. Rev. B* **82** 205315

[44] Gamble J K, Eriksson M A, Coppersmith S N and Friesen M 2013 *Phys. Rev. B* **88** 035310

[45] Zwanenburg F A, Dzurak A S, Morello A, Simmons M Y, Hollenberg L C L, Klimeck G, Rogge S, Coppersmith S N and Eriksson M A 2013 *Rev. Mod. Phys.* **85** 961

[46] Boross P, Széchenyi G, Culcer D and Pályi A 2016 *Phys. Rev. B* **94** 035438

[47] Tariq B and Hu X 2019 *Phys. Rev. B* **100** 125309

[48] Hosseinkhani A and Burkard G 2020 *Phys. Rev. Research* **2** 043180

[49] Lima J R F and Burkard G 2023 *Materials for Quantum Technology* **3** 025004

[50] Takashina K, Fujiwara A, Horiguchi S, Takahashi Y and Hirayama Y 2004 *Phys. Rev. B* **69** 161304

[51] Lai K, Lu T M, Pan W, Tsui D C, Lyon S, Liu J, Xie Y H, Mühlberger M and Schäffler F 2006 *Phys. Rev. B* **73** 161301

[52] Sasaki K, Masutomi R, Toyama K, Sawano K, Shiraki Y and Okamoto T 2009 *Appl. Phys. Lett.* **95** 222109

[53] Neyens S F, Foote R H, Thorgrimsson B, Knapp T J, McJunkin T, Vandersypen L M K, Amin P, Thomas N K, Clarke J S, Savage D E, Lagally M G, Friesen M, Coppersmith S N and Eriksson M A 2018 *Appl. Phys. Lett.* **112** 243107

[54] Abadillo-Uriel J C, Thorgrimsson B, Kim D, Smith L W, Simmons C B, Ward D R, Foote R H, Corrigan J, Savage D E, Lagally M G, Calderón M J, Coppersmith S N, Eriksson M A and Friesen M 2018 *Phys. Rev. B* **98** 165438

[55] Dodson J P, Ercan H E, Corrigan J, Losert M P, Holman N, McJunkin T, Edge L F, Friesen M, Coppersmith S N and Eriksson M A 2022 *Phys. Rev. Lett.* **128** 146802

[56] Ohkawa F J and Uemura Y 1977 *J. Phys. Soc. Jpn.* **43** 917

[57] Ohkawa F J 1978 *Solid State Commun.* **26** 69

[58] Valavanis A, Ikonić Z and Kelsall R W 2007 *Phys. Rev. B* **75** 205332

[59] Saraiva A L, Calderón M J, Hu X, Das Sarma S and Koiller B 2009 *Phys. Rev. B* **80** 081305

[60] Saraiva A L, Calderón M J, Capaz R B, Hu X, Das Sarma S and Koiller B 2011 *Phys. Rev. B* **84** 155320

[61] Wang L W and Zunger A 1995 *Phys. Rev. B* **51** 17398

[62] Wang L W, Kim J and Zunger A 1999 *Phys. Rev. B* **59** 5678

[63] Zhang S B, Yeh C Y and Zunger A 1993 *Phys. Rev. B* **48** 11204

[64] Kleinman L and Bylander D M 1982 *Phys. Rev. Lett.* **48** 1425

[65] Wang L and Zunger A 1994 *J. Chem. Phys.* **100** 2394

[66] Luo J W, Bester G and Zunger A 2009 *Phys. Rev. Lett.* **102** 056405

[67] Magri R and Zunger A 2002 *Phys. Rev. B* **65** 165302

[68] Wang L W, Franceschetti A and Zunger A 1997 *Phys. Rev. Lett.* **78** 2819

[69] An J M, Franceschetti A, Dudiy S V and Zunger A 2006 *Nano Lett.* **6** 2728

[70] Luo J W, Bester G and Zunger A 2009 *New J. Phys.* **11** 123024

[71] Pryor C, Kim J, Wang L W, Williamson A J and Zunger A 1998 *J. Appl. Phys.* **83** 2548

[72] Williamson A J, Wang L W and Zunger A 2000 *Phys. Rev. B* **62** 12963

[73] Weisstein E W *Rectangle function from MathWorld-A Wolfram Web Resource*

[74] Wang G, Song Z G, Luo J W and Li S S 2022 *Phys. Rev. B* **105** 165308

[75] McJunkin T, MacQuarrie E R, Tom L, Neyens S F, Dodson J P, Thorgrimsson B, Corrigan J, Ercan H E, Savage D E, Lagally M G, Joynt R, Coppersmith S N, Friesen M and Eriksson M A 2021 *Phys. Rev. B* **104** 085406